Mon. Not. R. Astron. Soc. **355,** 973–985 (2004) doi:10.1111/j.1365-2966.2004.08380.x

Connecting the cosmic infrared background to the X-ray background

L. Silva,[1⋆] R. Maiolino[2] and G. L. Granato[3]

[1]*INAF - Osservatorio Astronomico di Trieste, Via Tiepolo 11, I-34131 Trieste, Italy*
[2]*INAF - Osservatorio Astrofisico di Arcetri, Largo E. Fermi 5, I-50125 Firenze, Italy*
[3]*INAF - Osservatorio Astronomico di Padova, Vicolo dell'Osservatorio 5, I-35122 Padova, Italy*

Accepted 2004 September 2. Received 2004 September 1; in original form 2004 March 16

ABSTRACT

We estimate the contribution of active galactic nuclei (AGN) and of their host galaxies to the infrared background. We use the luminosity function and evolution of AGN recently determined by the hard X-ray surveys, and new spectral energy distributions connecting the X-ray and the infrared emission, divided in intervals of absorption. These two ingredients allow us to determine the contribution of AGN to the infrared background by using mostly observed quantities, with only minor assumptions. We find that AGN emission contributes little to the infrared background (<5 per cent over most of the infrared bands), implying that the latter is dominated by star formation. However, AGN host galaxies may contribute significantly to the infrared background, and more specifically 10–20 per cent in the 1–20 μm range and ∼5 per cent at $\lambda < 60$ μm. We also give the contribution of AGN and of their host galaxies to the source number counts in various infrared bands, focusing on those which will be observed with Spitzer. We also report a significant discrepancy between the expected contribution of AGN hosts to the submillimetre background and bright submillimetre number counts with the observational constraints. We discuss the causes and implications of this discrepancy and the possible effects on the Spitzer far-infrared bands.

Key words: galaxies: active – galaxies: starburst – cosmology: miscellaneous – infrared: galaxies – X-rays: galaxies.

1 INTRODUCTION

Active galactic nuclei (AGN) are known to be the main contributors to the cosmic X-ray background. Synthesis models suggested that the shape of the X-ray background requires a mixture of unabsorbed and absorbed AGN (Setti & Woltjer 1989; Comastri et al. 1995; Gilli, Salvati & Hasinger 2001). This scenario has been verified by the recent *Chandra* and *XMM–Newton* surveys which have resolved most of the X-ray background up to energies of 10 keV (Brandt et al. 2001; Giacconi et al. 2001; Hasinger et al. 2001). Indeed, the optical identification of the sources making the X-ray background, as well as their X-ray spectra, revealed both obscured and unobscured AGN, though unusual AGN were also identified (e.g. Mainieri et al. 2002; Barger et al. 2003; Fiore et al. 2003). The X-ray surveys have also provided evidence that the evolution of AGN is different with respect to that known from previous optical surveys. In particular, the evolution of low-luminosity AGN (in the Seyfert range) peaks at much lower redshift ($z < 0.5$) than for more luminous, quasi-stellar object (QSO)-like AGN (Hasinger 2003; Fiore et al. 2003; Ueda et al. 2003). This luminosity-dependent density evolution (LDDE) seems to apply both to unobscured and obscured AGN.

⋆E-mail: silva@ts.astro.it

The circumnuclear gas responsible for the X-ray absorption is associated with dust which absorbs the optical–ultraviolet (UV) radiation from the AGN and reprocesses it thermally into the infrared (IR). Dust infrared emission has been observed in all AGN (except in some BL Lacs and radio-loud quasars where the infrared radiation may be dominated by the relativistically boosted synchrotron radiation). At least in the near- and mid-IR, it has been recognized that a significant fraction of the dust radiation is due to heating by the AGN (e.g. Granato, Danese & Franceschini 1997; Maiolino et al. 1998a; Oliva et al. 1999; Glass 2004; Minezaki et al. 2004). For this reason it has been argued that AGN may contribute significantly also to the IR cosmic background. This issue is of utmost importance, since it would also have implications for the fraction of IR background which should be ascribed to star formation.

Some previous studies have estimated the contribution of AGN to the IR background or to the source number counts (Granato, Danese & Franceschini 1997; Matute et al. 2002; Risaliti, Elvis & Gilli 2002; Andreani, Spinoglio & Malkan 2003b).

The main ingredients for this estimate are the luminosity function (LF) and evolution of AGN and their spectral energy distribution (SED). Previous works have adopted the observationally available, still largely incomplete, LF of AGN, that only very recently has been better defined through *Chandra* and *XMM–Newton* surveys

(Ueda et al. 2003). Generally, a single template for the AGN SED has been assumed.

In this paper we investigate the contribution of AGN to the IR background and counts by using the most recent luminosity functions and evolution obtained by the recent hard X-ray surveys. We also use IR spectral energy distributions accurately derived by means of nuclear IR data for a sample of Seyfert galaxies (both obscured and unobscured) and which allow us to disentangle the AGN IR emission from the contribution of the host galaxy. These data also allow us to connect the IR emission of AGN directly to their intrinsic X-ray emission. Moreover, we use the novel approach of dividing the observed IR SEDs into intervals of different AGN obscuration, in terms of $N_{\rm H}$ along the line of sight. This is the same method adopted in the synthesis of the X-ray background. These various pieces of information combined together allow us to *connect the X-ray background (dominated by AGN) directly to the IR background without strong assumptions, by using only observed and measured quantities.*

Throughout the paper we adopt the following cosmological parameters: $H_0 = 70\,{\rm km\,s^{-1}\,Mpc^{-1}}$, $\Omega_{\rm m} = 0.3$ and $\Omega_\Lambda = 0.7$.

2 THE LUMINOSITY FUNCTION AND EVOLUTION OF AGN

The most recent results from the hard X-ray surveys (both shallow and deep) have been gathered by Ueda et al. (2003) to produce the hard X-ray luminosity function and evolution of AGN. These luminosity functions derived in the hard X-rays are optimal for our purposes, because they are much less affected by obscuration than the luminosity function derived at other wavelengths. Residual incompleteness in the fraction of heavily obscured AGN has been accounted for (see the discussion below for the case of Compton-thick AGN). Ueda et al. (2003) derive these quantities also by consistently requiring that the whole X-ray background is properly fitted. They also match the optical luminosity functions and evolution (Boyle et al. 2000) by assuming appropriate ratios between X-ray and optical luminosity.

We direct the reader to Ueda et al. (2003) for more details on their method and on the properties of their derived luminosity functions. Here we only summarize two important results of their work which are relevant for this paper. The density evolution of AGN is strongly dependent on their luminosity: the evolution of Seyfert galaxies peaks at a much lower redshift ($z \sim 0.3$–0.5) than the more luminous QSOs (whose evolution peaks beyond $z > 1$). The other important result is that the various observational constraints indicate that the fraction of obscured AGN decreases with luminosity. In particular, at high, QSO-like luminosities, the fraction of obscured AGN is lower by a factor of about 2 with respect to Seyfert nuclei.

In this paper we adopt the prescriptions by Ueda et al. (2003) for the luminosity functions, evolution and distribution in absorbing column densities $N_{\rm H}$, which properly reproduce the results from the X-ray surveys and the X-ray background. For Compton-thick sources with $10^{24} < N_{\rm H} < 10^{25}\,{\rm cm^{-2}}$, which contribute significantly to the 30-keV bump of the X-ray background, but which are poorly sampled by the current surveys at energies lower than 10 keV, we adopt the same strategy of Ueda et al. by assuming that their fraction is the same as for AGN with $10^{23} < N_{\rm H} < 10^{24}\,{\rm cm^{-2}}$ (consistent with the observations of local AGN, Risaliti, Maiolino & Salvati 1999). Ueda et al. (2003) also showed that this fraction of Compton-thick sources consistently reproduces the shape of the X-ray background (especially at 30 keV).

Compton-thick AGN with $N_{\rm H} > 10^{25}\,{\rm cm^{-2}}$ do not contribute significantly to the X-ray background at any energy, since they are totally absorbed and only their scattered component is observed, and therefore they are generally neglected in the synthesis models of the X-ray background. However, this class of heavily absorbed AGN could contribute significantly to the IR background and therefore this population must be included in our model. We assume that the fraction of Compton-thick AGN with $N_{\rm H} > 10^{25}\,{\rm cm^{-2}}$ is the same as those with $10^{24} < N_{\rm H} < 10^{25}\,{\rm cm^{-2}}$ and with $10^{23} < N_{\rm H} < 10^{24}\,{\rm cm^{-2}}$, again consistent with the observations of local AGN (Risaliti et al. 1999).

3 THE NUCLEAR INFRARED SPECTRAL ENERGY DISTRIBUTION

Various authors have derived the spectral energy distribution of AGN in the IR (e.g. Elvis et al. 1994; Spinoglio, Andreani & Malkan 2002; Alonso-Herrero et al. 2003; Kuraszkiewicz et al. 2003). However, in many cases their approach is not adequate for our purposes.

At least for what concerns Seyfert galaxies we need to know the nuclear infrared spectral energy distribution, i.e. the infrared light associated with the dust heated by the AGN and also direct AGN emission (at this stage without the contribution by the host galaxy). The infrared SED must be known both for unobscured AGN and for AGN obscured by various levels of obscuration, and even for the most obscured Compton-thick AGN. We need a large wavelength coverage, $\sim$1–1000 μm, in order to estimate the contribution of AGN to the near-IR-to-submillimetre background as well as to the source counts in the Spitzer, ISO and SCUBA bands. For each IR SED we also need to know its normalization in terms of *intrinsic* hard X-ray flux; this will allow us to link the IR SEDs to the hard X-ray luminosity functions.

3.1 Spectral energy distribution of Seyfert nuclei

We selected from the literature a large sample of Seyfert galaxies for which *nuclear* near-IR and mid-IR observations have detected clear signatures of *non-stellar* nuclear emission, and where the stellar contribution has been properly removed. Among these we only choose those objects having at least four nuclear photometric points[1] and at least one of them must be in the mid-IR (10 μm and/or 20 μm); such a minimum set of data is required for a proper interpolation with the models discussed below. We also required that the sources had hard X-ray measurements good enough to provide the intrinsic (i.e. unabsorbed) hard X-ray flux and a measure of the absorbing column density $N_{\rm H}$. In particular we require that the X-ray data allow a measurement of $N_{\rm H}$ with an accuracy of about 50 per cent at least, or that they allow one to set an upper limit on $N_{\rm H}$ below $10^{22}\,{\rm cm^{-2}}$ (below this value the absorption of the 2–10 keV luminosity is negligible). A total of 33 Seyfert nuclei matched these requirements (see Appendix A). Most of these Seyferts are from the Maiolino

[1] As mentioned above, by 'nuclear photometry' we mean the central non-stellar flux. In many works this flux is extracted through a spatial decomposition of the near/mid-IR images into a stellar light profile and a nuclear point-like source, or even spectroscopically (through the dilution of the stellar features, see reference in Appendix A). In cases where mid-IR images are not available (and only fixed aperture fluxes are available), if from the *K*-band image the nuclear source is found to dominate the light within the central few arcseconds, then it is assumed that also the mid-IR flux dominates within the same aperture (this is justified by the fact that the contrast between AGN hot-dust emission and stellar light is higher in the mid-IR).

& Rieke (1995) sample. The list of Seyferts used to derive the IR SEDs, along with the references for the data and some additional details, are given in Appendix A.

The nuclear IR data were then *interpolated* with the updated models of Granato & Danese (1994). These models were generated by means of a detailed radiative transfer code for dust heated by a nuclear central source with a typical AGN spectrum. The code includes various possible geometries and physics for the distribution of the circumnuclear dust (torus with variable height, radii and density, as well as tapered discs). The code also allows variation in the distribution of dust grain sizes, to account for possible deviations from the standard ISM extinction curve as suggested by some recent work (Maiolino, Marconi & Oliva 2001; Maiolino et al. 2001; Gaskell et al. 2004). There are several other models which have been proposed to describe the circumnuclear dust emission in AGN (e.g. Pier & Krolik 1993; Efstathiou & Rowan-Robinson 1995; Nenkova, Ivezić & Elitzur 2002). However, we do not want to discuss here the different features of the various models and which of them may be more appropriate to describe the properties of the circumnuclear dust in AGN. In this paper the models are simply used to interpolate the observed nuclear IR data with a physically plausible SED. As long as the latter is constrained by the data, the choice of the specific model does not change the results concerning the interpolated spectral region, typically within $\sim$2–20 μm.

More critical is the *extrapolation* of the models beyond 20 μm, where nuclear IR data are not available (only large-aperture data from ISO or IRAS are available at $\lambda > 20\,\mu$m). In this spectral region there is some degeneracy among models. Our best-fitting models (for each individual AGN of our sample) generally suggest a drop of the IR emission redward of $\sim$30–50 μm. Some authors propose models which fit relatively flat SEDs to data up to 100 μm (Andreani, Franceschini & Granato 1999; Kuraszkiewicz et al. 2003). As discussed in several works on IR emission by AGN, mid-infrared (MIR) data are generally better reproduced by models in which the SED drops in the far-infrared (FIR; e.g. Granato & Danese 1994; Efstathiou & Rowan-Robinson 1995; Galliano et al. 2003). Moreover those models with relatively flat FIR SEDs would require the existence of very extended dusty torii ($\sim$1–10 kpc, e.g. Andreani et al. 1999). This is difficult to justify, and in any case, it has been excluded at least for NGC 1068, whose torus has been directly observed (Jaffe et al. 2004).

However, the far-IR part of our nuclear AGN SEDs remains subject to strong uncertainties and is admittedly model dependent.

The SEDs of the single objects were then normalized by the intrinsic, unabsorbed X-ray flux in the 2-10 keV band. Note that this prevents us using objects with $N_{\rm H} > 10^{25}\,{\rm cm}^{-2}$ (such as NGC 1068, Matt et al. 1997), because their X-ray radiation is totally absorbed at all energies and therefore the intrinsic X-ray emissions cannot be recovered. The issue of the inclusion of this class of objects in our model will be discussed in Section 5.

The X-ray-normalized infrared SEDs were then divided into intervals of absorption in terms of $N_{\rm H}$. We do not enter into the issue of the mismatch between gas absorption in the X-rays and dust absorption in the optical/infrared (Maiolino et al. 2001) and, more specifically, that dust absorption is generally significantly lower than expected by a Galactic dust-to-gas ratio and by a Galactic extinction curve. Regardless of such physical issues, we simply follow the phenomenological approach of dividing the AGN in terms of $N_{\rm H}$; this will then allow us to match the *observationally* more adequate IR SED properly to each class of absorbed AGN used to synthesize the X-ray background. The resulting average infrared SEDs are shown in Fig. 1. Note that in our sample of Sy2 there are no objects with $10^{21} < N_{\rm H} < 10^{22}\,{\rm cm}^{-2}$; the inclusion of this class of AGN (which is only a minor fraction of the whole population, as found both locally and in the hard X-ray surveys, Risaliti et al. 1999; Ueda et al. 2003) will be discussed in Section 5.

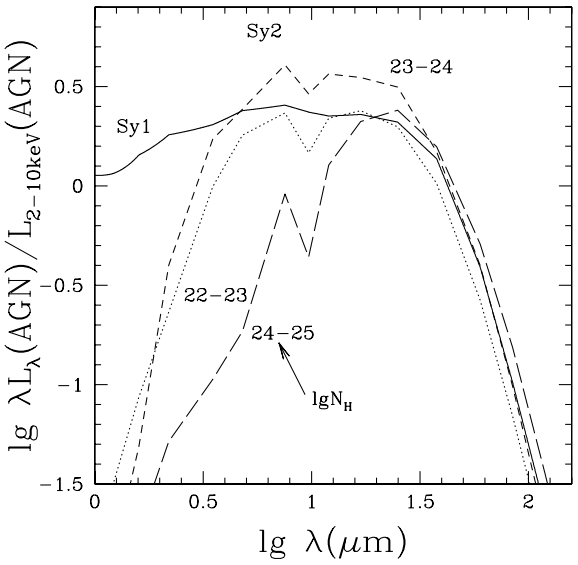

Figure 1. Nuclear (AGN only) infrared spectral energy distributions of Seyfert galaxies, normalized to the hard X-ray (2–10 keV) intrinsic luminosity and averaged within bins of absorbing $N_{\rm H}$. The solid line is the SED for Sy1s, the dotted line for Sy2s with $10^{22} < N_{\rm H} < 10^{23}\,{\rm cm}^{-2}$, the short-dashed line for Sy2s with $10^{23} < N_{\rm H} < 10^{24}\,{\rm cm}^{-2}$ and the long-dashed line is for Sy2s with $10^{24} < N_{\rm H} < 10^{25}\,{\rm cm}^{-2}$.

The main difference between the SEDs of Sy1s and the SEDs of Sy2s with $10^{22} < N_{\rm H} < 10^{23}\,{\rm cm}^{-2}$ is absorption in the near-IR at $\lambda \lesssim 2\,\mu$m and some mild silicate absorption at 9.7 μm. For Sy2s with $10^{23} < N_{\rm H} < 10^{24}\,{\rm cm}^{-2}$ the shape of the IR SED does not change significantly except for a slight, overall increase of the emission. The finding that the shape of the IR SED remains unchanged indicates that the medium absorbing the X-rays with $N_{\rm H} \sim 10^{23.5}\,{\rm cm}^{-2}$ is either too small in size to obscure the near-IR emitting region or that its dust content/composition is unable to effectively absorb the near-IR radiation. The slight increase of the overall IR emission might indicate a slight increase of the covering factor of the circumnuclear dust. However, one should keep in mind that the number of objects used to create the average SEDs is still small and therefore statistical fluctuations may still be significant. For Compton-thick Sy2s ($N_{\rm H} > 10^{24}\,{\rm cm}^{-2}$) the IR SED is significantly different, showing a prominent absorption even in the mid-IR (although still much lower than expected by the dust associated with a Compton-thick medium and with a Galactic gas-to-dust ratio and composition).

3.2 Spectral energy distribution of quasars

Disentangling the nuclear infrared emission from the contribution of the host galaxy is a much more difficult task for quasars. Indeed at their larger distances, even small apertures include a significant fraction of the host galaxy. Resolving the host galaxies in several quasars has been achieved by various authors in the near-IR (McLeod & Rieke 1994a,b; Surace, Sanders & Evans 2001), but at longer wavelengths ($\lambda \geqslant 3\,\mu$m) we still have integrated information. Moreover, infrared data are generally available for unobscured quasars, while there is little information on the IR emission of the few Type 2 quasars known. For these reasons we assume that the

shape of the infrared emission as a function of the obscuration is the same as for the Seyfert nuclei.

However, the normalization to the X-ray flux cannot be assumed to be the same, since it is known that the X-ray radiation decreases relative to (at least) the optical–UV radiation at high luminosities. To determine the normalization factor we adopt again an observational approach. We merged the samples of quasars measured in the infrared by Andreani et al. (1999, 2003a) and Haas et al. (2000, 2003). These samples are all selected in the optical and, therefore, include only unobscured quasars. We selected only those quasars having at least four IR detections, at least one of which is in the far-IR, thus allowing a proper determination of their total IR SED. The latter criterion may bias our sample in favour of IR-bright quasars and with excess of star formation, as discussed below. We further selected only those quasars which also have X-ray measurements (good enough to ensure that there is no significant $N_{\rm H}$ absorption affecting the observed $L_{2-10\,{\rm keV}}$). Then we assume that at 12 μm the QSO integrated radiation is dominated by the QSO light, which is a reasonable approximation, since at this wavelength the AGN radiation is strong while the radiation from the galaxy is close to its minimum. We determine the average ratio $\lambda F_\lambda(12\,\mu{\rm m})/F(2\text{–}10\,{\rm keV})$ for all quasars in our sample and use this quantity to scale the SED derived for Sy1s relative to the X-ray emission. Then the SEDs of obscured quasars are derived from the SEDs of Sy2s by rescaling them to maintain the same intensity relative to unobscured quasars (i.e. the same relative intensities shown in Fig. 1). The average ratio $\lambda F_\lambda(12\,\mu{\rm m})/F(2\text{–}10\,{\rm keV}) = 3.6$ derived for quasars is only a factor 1.4 higher than for Sy1s (2.5). This result may sound odd, since when looking at the optical–UV bands the ratio F(opt)/F(X) is higher by a factor of three in quasars relative to Seyferts. Our finding suggests that the covering factor of dust is lower at higher luminosities, which reduces the overall IR flux relative to the optical radiation. This issue has been briefly discussed in Maiolino (2002) and will be subject of a forthcoming more detailed paper (Maiolino & Granato, in preparation). This finding is also in agreement with the recent results by Ueda et al. (2003) and by Hasinger (2003) who find that the fraction of obscured AGN at high, quasar-like luminosities is lower than in Seyferts.

4 THE TOTAL INFRARED SPECTRAL ENERGY DISTRIBUTION OF AGN AND OF THEIR HOST GALAXIES

We have also investigated the contribution by the host galaxies of AGN. This is a more uncertain investigation since it relies on the assumption that the relation between host galaxy and nuclear emission is, at high redshift, the same as observed in local galaxies.

The additional problem is that our method requires a proportionality between infrared SED and X-ray luminosity. There is no reason, in principle, to assume that the host galaxy infrared light is proportional to the AGN-dominated X-ray light (this is a conceptual problem also of other works, as discussed in Section 7). However, various studies have shown that the two phenomena, star formation and AGN, are related and must yield to the well-known correlation between black hole mass and bulge mass (Ferrarese & Merritt 2000; Marconi & Hunt 2003). In particular, Croom et al. (2002) found that the *optical* luminosity of the host galaxy scales as $L_{\rm host} \propto L_{\rm QSO}^{0.4}$, although with a large scatter. We therefore investigated the SEDs of the host galaxies as a function of the (X-ray) luminosity of the active nucleus.

We collected all infrared measurements which, especially for Seyferts, include the contribution of both the nucleus and the host galaxy (e.g. IRAS and 2MASS total photometry). We then subtracted from the integrated photometric points the contribution of the nucleus estimated as discussed in Section 3. The residuals were then fitted with galaxy models (a combination of active and quiescent stellar populations) obtained with the publicly available code GRASIL[2] (Silva et al. 1998).

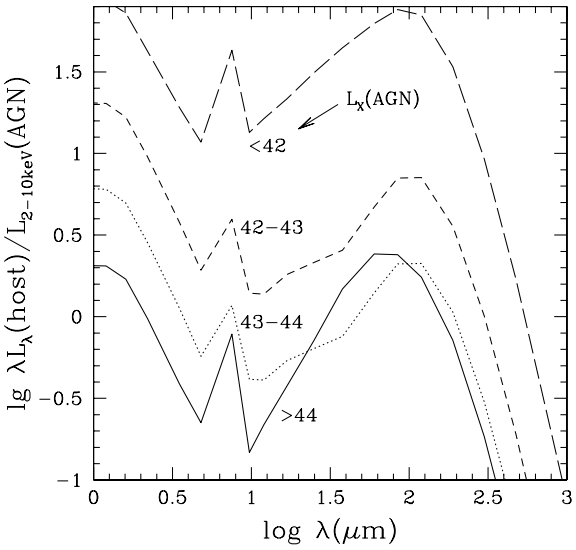

Figure 2. Infrared SED of Seyfert host galaxies normalized to the X-ray luminosity of the AGN. The SED have been divided in bins of X-ray luminosity and averaged. The solid line is the SED of galaxies hosting AGN with $L_{2-10\,{\rm keV}} > 10^{44}\,{\rm erg\,s^{-1}}$, dotted for galaxies hosting AGN with $10^{43} < L_{2-10\,{\rm keV}} < 10^{44}\,{\rm erg\,s^{-1}}$, short-dashed for galaxies hosting AGN with $10^{42} < L_{2-10\,{\rm keV}} < 10^{43}\,{\rm erg\,s^{-1}}$ and long-dashed for galaxies hosting AGN with $L_{2-10\,{\rm keV}} < 10^{42}\,{\rm erg\,s^{-1}}$

The resulting SEDs of the host galaxies were normalized by the X-ray luminosity of the nucleus (which is required to link the SEDs to the AGN evolution and luminosity functions), grouped in intervals of luminosity and then averaged within each group.

Fig. 2 shows the infrared SEDs of the host galaxies, normalized to the X-ray luminosity, and averaged within various ranges of $L_{\rm X}$. As expected the host galaxy contribution relative to the active nucleus decreases at higher AGN luminosities. At quasar-like luminosities ($L_{\rm X} > 10^{44}\,{\rm erg\,s^{-1}}$) the luminosity of the host decreases in the near-IR but not significantly in the far-IR. This may indicate that the hosts of high-luminosity AGN are undergoing enhanced star formation, similar to that found by the SDSS (Kauffmann et al. 2003), but may also be a bias due to our selection criterion for quasars in our sample (Section 3.2).

The total SEDs were simply obtained by combining the nuclear SED (Section 3) and the SEDs from the host galaxies for each range of luminosity ($L_{\rm X}$) and AGN absorption ($N_{\rm H}$).

5 CONNECTING THE INFRARED AND X-RAY BACKGROUND

The IR SEDs divided into groups based on their level of absorption and normalized to the hard X-ray flux, along with the hard X-ray

[2] The executable and a set of galaxy SEDs including those presented in Silva et al. (1998) can be downloaded at http://adlibitum.oat.ts.astro.it/silva/default.html or http://web.pd.astro.it/granato/

luminosity functions and evolution by Ueda et al. (2003), provide us with all the information needed to connect the X-ray cosmic background to the infrared background.

For AGN with (mild) absorption in the range $10^{21} < N_{\rm H} < 10^{22}\,{\rm cm}^{-2}$ we have no IR SED (see Appendix A), since this is a rare class of AGN in the local Universe and therefore there are no representatives in our sample. However at $N_{\rm H} < 10^{22}\,{\rm cm}^{-2}$, even for a Galactic dust-to-gas ratio, the absorption in the IR is negligible (less than 0.2 mag even in the 2-μm band). Therefore, for this class of AGN we assume the same IR SED as a Type 1 Seyfert, and with the optical direct component absorbed (yet the optical spectrum is not of interest since it is not investigated in this paper).

Compton-thick AGN absorbed by $N_{\rm H} > 10^{25}\,{\rm cm}^{-2}$ are not included in Ueda et al. (2003) because their contribution to the X-ray background is negligible (totally absorbed at all energies and only a weak reflection component is observed in the X-rays). However, their reprocessed radiation is observed in the infrared (the stereotype case is NGC 1068). As discussed in Section 3, we cannot derive the IR SED of this class of object normalized to the X-ray emission just because it is not possible to measure their intrinsic X-ray luminosity (and anyhow only NGC 1068 has the required data to derive a nuclear IR SED). Therefore we assume that absorbed AGN with $N_{\rm H} > 10^{25}\,{\rm cm}^{-2}$ have the same IR SED as the AGN with $10^{25} > N_{\rm H} > 10^{24}\,{\rm cm}^{-2}$ both in terms of shape and in terms of normalization relative to the intrinsic X-ray emission. We further assume, based on the $N_{\rm H}$ distribution of local Seyferts (Risaliti et al. 1999), that the fraction of AGN with $N_{\rm H} > 10^{25}\,{\rm cm}^{-2}$ is the same as the fraction of AGN with $10^{25} > N_{\rm H} > 10^{24}\,{\rm cm}^{-2}$.

Another issue is the definition of the dividing luminosity between 'Seyferts' and 'quasars', i.e. what are the luminosity ranges where the two different classes of SEDs should be used? This issue is actually of little importance since as discussed in Section 3.2 the nuclear SEDs for Seyferts and quasars are nearly identical (just 40 per cent difference in the normalization). Traditionally, in the X-rays the dividing luminosity is taken at about $10^{44}\,{\rm erg\,s}^{-1}$ in the 2–10 keV band, which roughly corresponds to a bolometric luminosity of $10^{45}\,{\rm erg\,s}^{-1}$. The luminosity of $L_{2-10\,{\rm keV}} = 10^{44}\,{\rm erg\,s}^{-1}$ appears to be an adequate dividing luminosity also for the Seyfert 1s and the quasars in our samples (see Appendix A), and therefore we will consistently use this dividing luminosity.

To compare the contribution of AGN to the IR bands with that due to normal/starburst galaxies (i.e. galaxies powered only by stars), we have also included the contribution by the latter, as described by Silva et al. (2004). There, the galaxy populations accounted for are spheroidal galaxies (based on the model by Granato et al. 2004), and late-type galaxies (spirals and starbursts). We refer to the cited papers for more details.

6 RESULTS

6.1 The contribution of AGN to the infrared background

Our estimated contribution of AGN (without hosts) to the IR background is shown in Fig. 3.

The main result is that AGN contribute little to the overall IR background. The spectral region where some significant AGN contribution is found (3 to ∼5 per cent) is between 5 μm and 40 μm. At wavelengths just below 10 μm, the background due to galaxies shows a leap that causes a maximum ($\gtrsim$10 per cent) for the contribution of AGN. But that leap is mostly due to the transition between the evolutionary regime assumed for late-type galaxies in the MIR-to-submillimetre region and in the near-infrared (NIR; see Silva et al. 2004)

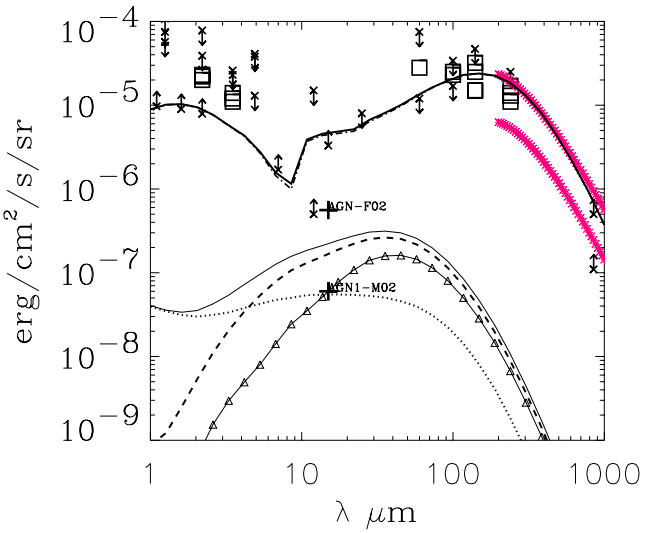

Figure 3. The IR background. The contribution due to the nuclear emission by AGN is shown by the thin continuous line. The dotted and dashed lines show the contribution by Type 1 and 2 AGN, respectively. The connected triangles show the contribution by Compton-thick nuclei ($N_{\rm H} > 10^{24}$ cm^{-2}). The IR background due to galaxies is shown by the dot-dashed line. Observational data for the IR background are from Hauser & Dwek (2001). The thick crosses show the contribution to the 15-μm background estimated for Type 1 AGN by Matute et al. (2002), and for total AGN by Fadda et al. (2002).

At all infrared wavelengths $\lambda > 5$ μm the AGN contribution is dominated by heavily obscured Seyfert nuclei ($N_{\rm H} > 10^{23}\,{\rm cm}^{-2}$), in particular at $\lambda > 20$ μm the contribution is dominated by Compton-thick Seyferts ($N_{\rm H} > 10^{24}\,{\rm cm}^{-2}$).

In Fig. 3 we also show the contribution of AGN to the 15-μm background inferred by Fadda et al. (2002) and by Matute et al. (2002) (limited to Type 1 AGN only) based on the cross-correlation between hard X-ray sources and mid-IR ISO sources or through direct optical identification of the ISO sources. These values are higher than predicted by our model because the ISO sources also include the contribution by the host galaxies. Therefore the comparison with these results will be discussed in the next section.

We point out that recently growing evidence has been found for a class of totally buried and optically elusive AGN in nearby galaxies (Marconi et al. 2000; Della Ceca et al. 2002; Maiolino et al. 2003). This class of AGN may be as numerous as classical, optically identified AGN. Most of them are Compton-thick and therefore, if they are present also at high redshift, they would mostly be missed even by current hard X-ray surveys. On the other hand their IR emission would provide an additional contribution to the IR background, which at the current stage is not included in our model.

We also recall that, as described in Section 3, the far-IR nuclear SEDs of AGN are not directly observed, therefore our estimated background in that spectral region is subject to higher uncertainties as compared to the near and mid-IR.

The contribution of AGN to the IR source counts is discussed only for the case of the AGN + host SEDs in the next section, since available data refer to the total emission of sources.

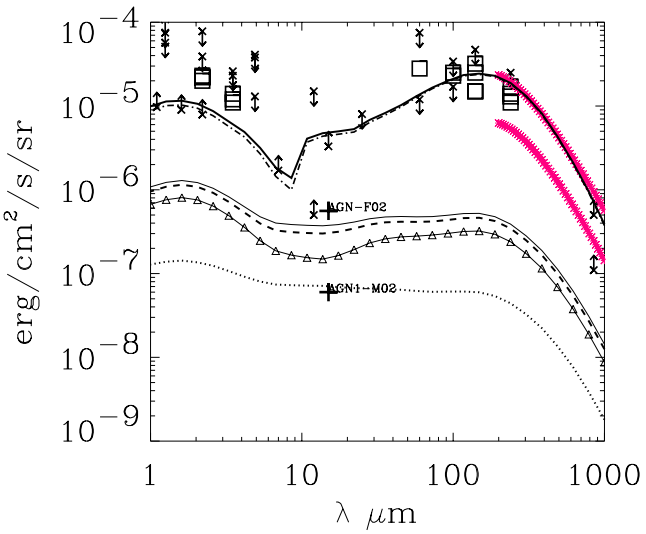

Figure 4. The IR background. The contribution due to the emission by the AGN plus their host galaxies is shown by the thin continuous line. The dotted and dashed lines show the contribution by Type 1 and 2 AGN + hosts, respectively. The connected triangles show the contribution by Compton-thick systems ($N_{\rm H} > 10^{24}$ cm^{-2}). The IR background due to galaxies, the same as in Fig. 3, is shown by the dot-dashed line. Observational data for the IR background are from Hauser & Dwek (2001). The thick crosses show the contribution to the 15-μm background estimated for Type 1 AGN by Matute et al. (2002), and for total AGN by Fadda et al. (2002).

6.2 The contribution of AGN *and* of their host galaxies to the infrared background

When the contribution by the host galaxy is included, the fraction of the IR background ascribed to AGN + hosts is much higher. This is shown in Fig. 4.

The overall contribution is larger than 5 per cent at all infrared wavelengths $\lambda < 40$ μm, and reaches about $\gtrsim$10 per cent for $\lambda \leqslant 10$ μm. The contribution at 15 μm is nearly two times higher with respect to the case of AGN alone (i.e. AGN and their host galaxies contribute nearly equally at this wavelength). The AGN + host contribution decreases at longer wavelengths, but is still a few per cent even in the submillimetre. The dominant contribution is due to the host galaxies of Compton-thick AGN.

The comparison of our model with the AGN contribution at 15 μm observationally inferred by various studies is reasonably good. The sum of the contribution by Type 1 Sys and QSOs at 15 μm expected by our model matches perfectly the value obtained by Matute et al. (2002) by the direct identification of the ISO sources (an identification survey which should be free of selection effects given that Type 1 AGN are unobscured and therefore easier to identify). Our estimated total AGN contribution to the 15-μm background is also close to that inferred by Fadda et al. (2002), though slightly lower. The slight difference with Fadda et al. (2002) may be due to a shortage of Seyfert galaxies at high redshift in the adopted luminosity function; indeed Ueda et al. (2003) may be slightly incomplete in this regard since the constraints on the fraction of Seyfert galaxies at high redshift are looser. We will discuss this issue again below.

By cross-correlating the *Chandra*/*XMM–Newton* sources with the submillimetre sources, various authors have estimated that AGN contribute about 7–15 per cent to the submillimetre background, depending on the X-ray flux limit reached (Severgnini et al. 2000; Barger et al. 2001). Our model predicts a significantly lower contribution (∼3 per cent) at 850 μm by the host galaxies. Again, this inconsistency is probably due to a shortage of Seyfert galaxies at high redshift in the luminosity function by Ueda et al. (2003). This will be discussed in more detail below when presenting the source number counts.

Figs 5–8 show the source number counts at various infrared wavelengths.

Note that for galaxies we have maintained the same prescriptions adopted in the previous section, while in principle we should decrease their contribution since part of the star formation is already accounted for through the host galaxies of AGN. But, apart from a slight overestimate of the bright 15-μm differential counts (Fig. 6), the models are still within the available observational constraints, therefore we keep the model for galaxies without modifications. This can introduce a slight underestimate of the relative importance of the hosts of AGN at bright fluxes.

The contribution by AGN + hosts is considerable at all wavelengths shortward of ∼100 μm, exceeding 10 per cent at intermediate-to-bright fluxes ($S \gtrsim 0.1$–1 mJy).

In the well-studied band at 15 μm AGN + hosts dominate the counts at fluxes higher than a few mJy (the AGN + hosts contribution is ∼10, 30, 40 and 60 per cent, respectively at flux levels of 0.1, 1, 5 and 100 mJy, Fig. 6). Qualitatively our finding is in agreement with the recent study by La Franca et al. (2004) whose optical identification of the ISO 15-μm sources (combined with their preliminary results on X-ray identifications, La Franca et al., in preparation) indicate a rapidly increasing fraction of AGN at high fluxes. Quantitatively La Franca et al. (2004) find only half of the AGN expected by our model, but the statistical error bars are actually consistent with our values at the 1σ level. However, if one wishes to investigate this marginal inconsistency, one possibility, as suggested by La Franca et al. (2004), could be that optical spectroscopic identifications have missed a significant fraction of Type 2 AGN. Our model indicates that most of the AGN contributing to the source counts are heavily obscured (Compton-thick) and therefore are more likely to be missed by optical identification. In particular, Maiolino et al. (2003) have clearly shown that several Compton-thick AGN have been missed by optical spectroscopy even in nearby galaxies. La Franca et al. (in preparation) attempt to account for such optically elusive AGN by exploiting the current results in this regard from X-ray surveys. None the less as pointed out both by Ueda et al. (2003) and by Maiolino et al. (2003) most such Compton-thick AGN are probably missed even by the latest hard X-ray surveys. Another possibility, as suggested by the comparison with La Franca et al. (2004), is that the extrapolation of the luminosity functions by Ueda et al. (2003) tend to overestimate the density of AGN at low redshift.

A much more critical issue is the contribution of AGN to the number counts at 850 μm. Alexander et al. (2003) have found that about half of the submillimetre sources brighter than 5 mJy host a Seyfert nucleus. In more recent work, Alexander et al. (2004) identify most of these sources as galaxies at $z \sim 2$ (i.e. at a redshift comparable with most of the submillimetre sources at this limiting flux). Our model predicts that only a few per cent of the submillimetre sources host an AGN at fluxes $S_{850\,\mu{\rm m}} > 5$ mJy. Again, the main problem seems to be that the luminosity functions of Ueda et al. (2003) underestimate the number of Seyfert galaxies at high redshift.

Indeed, at $z > 2$ the luminosity function at Seyfert luminosities is not tightly constrained by the observational data available to Ueda et al. (2003) and therefore it is mostly extrapolated from lower redshifts. This issue may also affect our estimated contribution of AGN

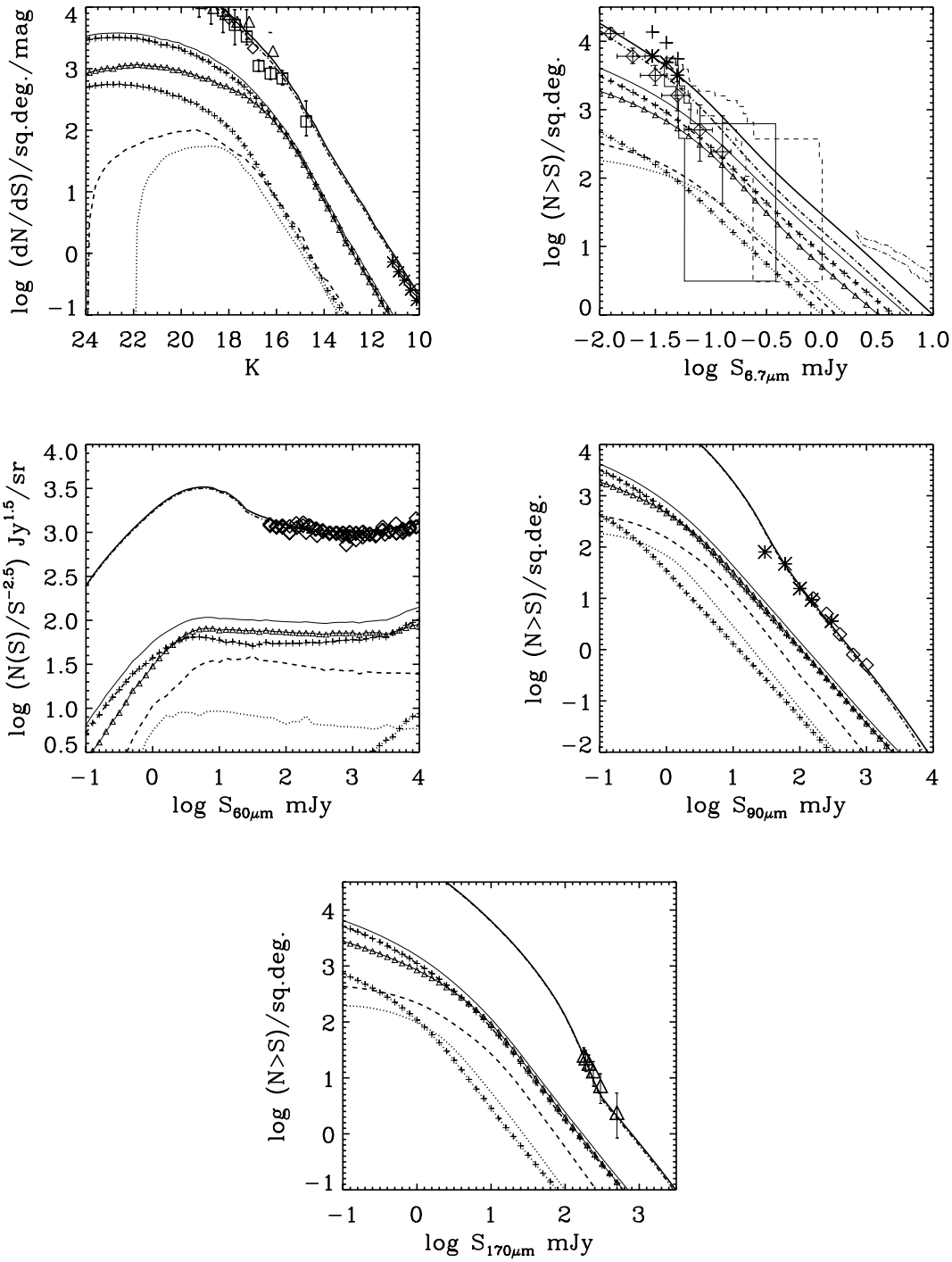

Figure 5. Number counts for AGN + hosts and galaxies in several NIR to FIR bands where data are available. Meaning of lines is: thin continuous for AGN + their host galaxies; dotted and dashed for Type 1 and 2 QSOs + hosts, respectively; the same line styles with plus signs superimposed are for Type 1 and 2 Seyferts + hosts; the connected triangles show the contribution by Compton-thick AGN ($N_{\rm H} > 10^{24}$ cm^{-2}); dot-dashed line for galaxies. Data are from: Moustakas et al. (1997), Kochanek et al. (2001), Saracco et al. (2001), Totani et al. (2001), and Cimatti et al. (2002) (*K* band); Taniguchi et al. (1997), Altieri et al. (1999), Serjeant et al. (2000), Oliver et al. (1997) (closed region with continuous line), Oliver et al. (2002) (closed region with dashed line), and Sato et al. (2003) (6.7 μm); Lonsdale et al. (1990), Pearson & Rowan-Robinson (1996), Bertin, Dennefeld & Moshir (1997), Mazzei et al. (2001) (60 μm); Efstathiou et al. (2000), Rodichiero et al. (2003) (90 μm); Dole et al. (2001) (170 μm).

hosts to the far-IR bands of Spitzer. A more detailed investigation of this issue and of the possible implications for the evolution of Seyferts at high redshift will be discussed in an upcoming paper (Silva et al. in preparation). An additional problem might be our modelling of the host SEDs in the submillimetre. Indeed, due to the lack of submillimetre data for most of the sources in our sample, the long-wavelength tails of the SEDs in Fig. 2 are mostly obtained by extrapolating the far-IR data with theoretical models which fit properly the SEDs of local starburst and quiescent galaxies. However, such extrapolation may be wrong by some factor.

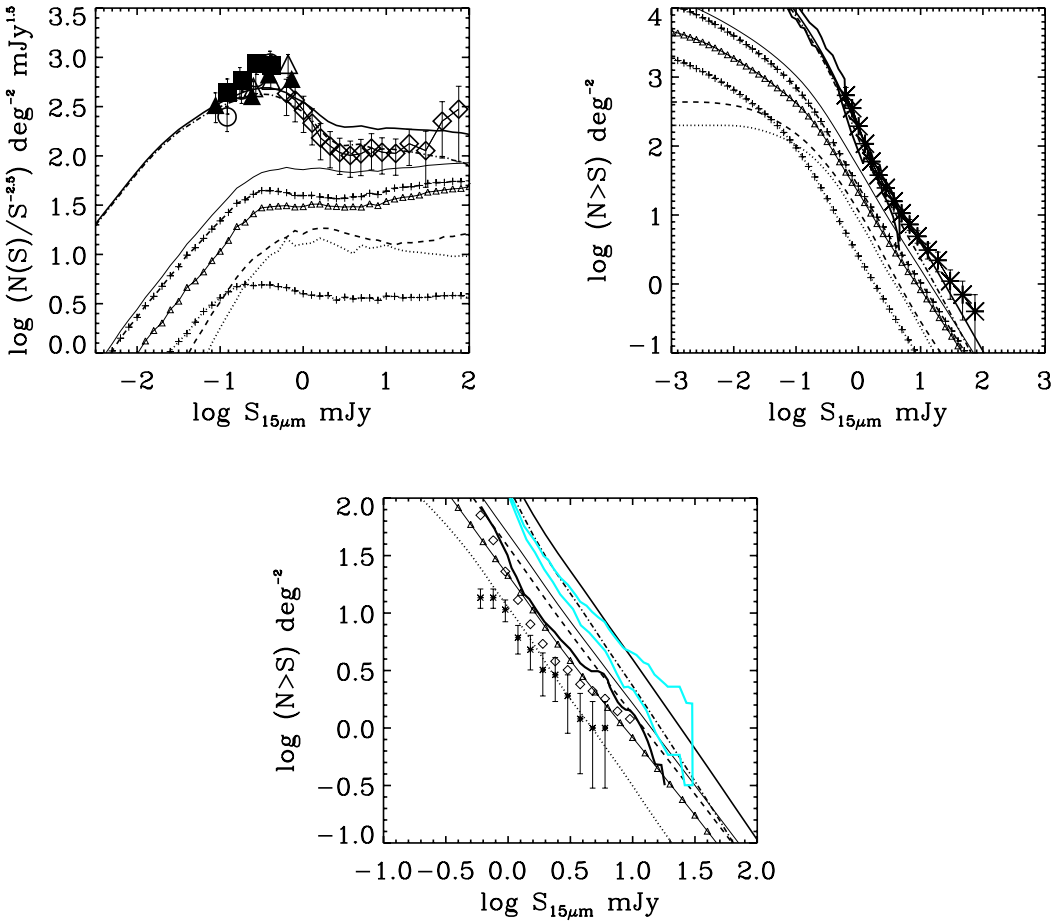

Figure 6. 15-μm number counts for AGN + hosts and galaxies. Meaning of lines as in Fig. 5. In the upper two plots data are from Elbaz et al. (1999) and Gruppioni et al. (2002). In the lowest plot, the integral 15 μm counts are compared with data by La Franca et al. (2004) and La Franca et al. (in preparation), that have evaluated the source counts due to Type 1 and 2 AGN by means of optical and X-ray identifications of the 15-μm sources. In this plot, data for Type 1, Type 2 and total AGN, and the total counts are shown, respectively, by asterisks, diamonds, the thick line and the the closed region. The corresponding quantities for our model are shown by the dotted, dashed, the thin and the thick continuous line. The connected triangles show the contribution by Compton-thick sources.

In the Spitzer bands with $\lambda \leqslant 24$ μm we expect that important fractions of the total detected sources will be provided by galaxies hosting an AGN. This is particularly true at bright flux limits. At the sensitivity limits reported by Lonsdale et al. (2003) for the SWIRE survey (7.3, 9.7, 27.5, 32.5 μJy, respectively, for the IRAC 3.6, 4.5, 5.8, 8 μm bands, and 0.45 mJy for the 24-μm band of MIPS), we get that ∼7–25 per cent of the total sources host AGN, with the maximum value at 5.8 and 8 μm.

At the longer MIPS bands, 70 and 160 μm, at flux limits in the ranges ∼5–10 mJy, and ∼70–100 mJy, respectively, we expect that only a few per cent of the detected sources will host an AGN. However, at these long wavelengths our estimates may be affected by the same problem as for the submillimetre sources as a consequence of the shortage of high-z Seyferts in the Ueda et al. (2003) model.

7 COMPARISON WITH PREVIOUS STUDIES

In the previous section we have compared the predictions of our model with observational constraints at specific wavelengths. However, the contribution of AGN to the IR background and IR number counts has been modelled and investigated by other authors in the past. In this section we compare our results with some of these previous studies.

In Granato et al. (1997), predictions for the contribution of AGN to the IR background and MIR source counts were presented, starting from the X-ray background as a constraint. Theoretical nuclear SEDs as a function of $N_{\rm H}$ were used for AGN, and the contribution by the host galaxy was considered in a very approximate manner. Their results are within a factor of 2 as compared to ours for the nuclear emission by AGN in the ∼6–90 μm range. The reason is that they assumed that the MIR SEDs are ascribed to the AGN only.

Starting from their observed contribution to the 15-μm background from Type 1 AGN, Matute et al. (2002) infer the total contribution from all AGN to the 15-μm background. Under 'standard' assumptions based on unified theories they infer a total contribution of ∼10–15 per cent, which is similar to that inferred by us.

Risaliti et al. (2002) predict that the maximum contribution from AGN to the infrared background occurs at 60 μm and at the level of 20–40 per cent. This is significantly different from that predicted by our model, which predicts a maximum contribution by AGN + hosts at about 10 μm and not exceeding 20 per cent. However, there are two main problems in Risaliti et al. (2002). First, they assume the bolometric correction (the proportionality between $L_{\rm X}$ and $L_{\rm bol}$) typical of quasars, while it is now known that a large fraction of the X-ray background is produced at Seyfert-like

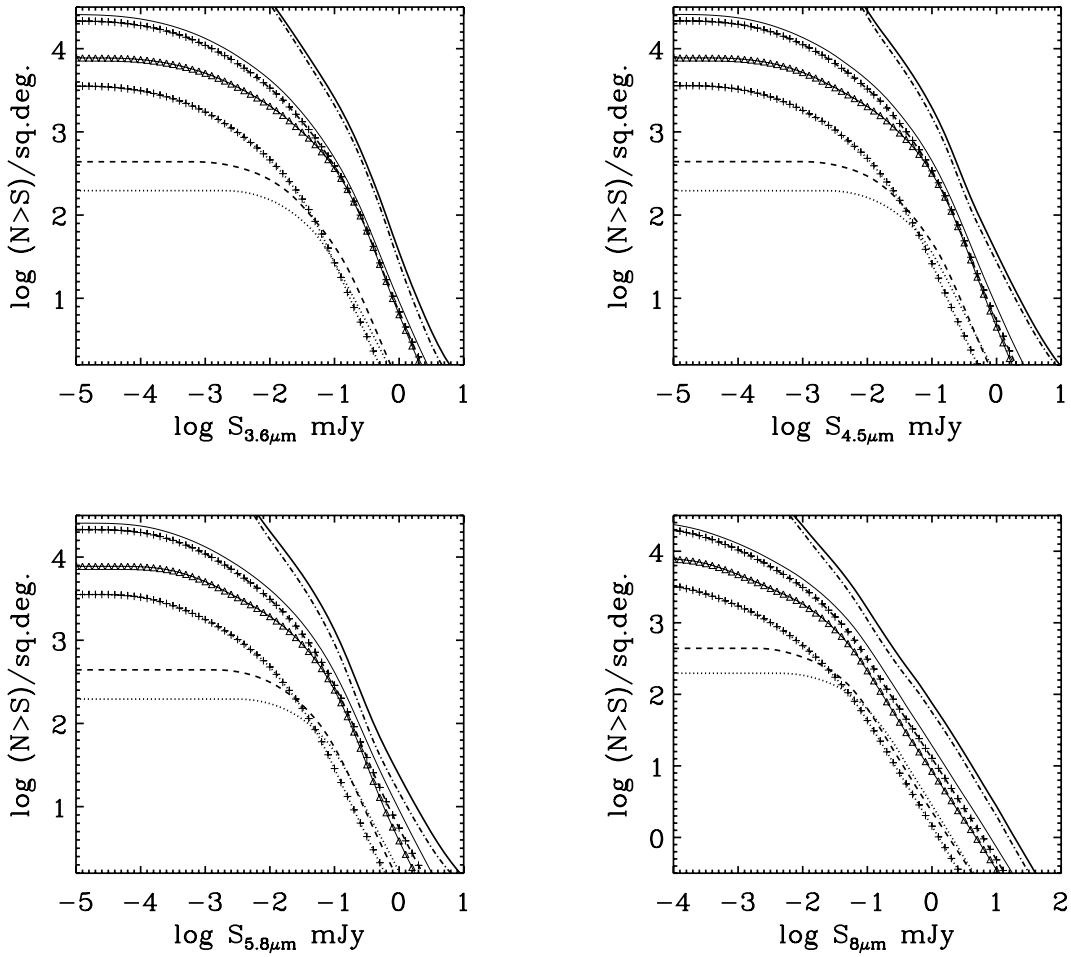

Figure 7. Number counts for AGN + hosts and galaxies in the Spitzer/IRAC bands. Meaning of lines is: thin continuous for AGN + their host galaxies; dotted and dashed for the hosts of Type 1 and 2 QSOs, respectively; the same line styles with plus signs superimposed are for Type 1 and 2 Seyferts; the connected triangles show the contribution by Compton-thick AGN ($N_{\rm H} > 10^{24}$ cm^{-2}); dot-dashed line for galaxies.

luminosities (for which the bolometric correction is lower by a factor of about 3). Secondly, they assume that most of the quasars are absorbed (80–90 per cent), while recently it has become clear that at quasar luminosities the fraction of obscured AGN is much lower than for Seyferts, and more specifically the fraction of obscured AGN at $L_{\rm X} > 10^{44}$ erg s^{-1} is only 30–40 per cent. These two factors are mostly responsible for the excess of IR background ascribed to AGN in Risaliti et al. (2002).

More recently Andreani et al. (2003b) have derived the contribution of various classes of active galaxies to the source number counts in different infrared bands. They consider separately the contribution by Sy1s, Sy2s and QSO1s (but not QSO2s) and use the SEDs inferred by Spinoglio et al. (2002) which include the contribution from the host galaxies. Therefore, their predictions should be comparable with our results in Section 6.2. They adopt pure luminosity evolutions from Malkan & Stecker (2001) and Boyle et al. (2000). It is now clear that AGN follow a luminosity-dependent density evolution (LDDE), however pure luminosity evolution formulas provide a reasonable approximation for the behaviour of the bulk of AGN around the knee of the luminosity function and above. The predictions of the source number counts obtained by Andreani et al. (2003b) in the various IR bands are close to those obtained by us, at least for what concerns the *total* AGN contribution. Yet, our model predicts a larger contribution by obscured (Type 2) AGN than predicted by Andreani et al. (2003b). In this regard, one should keep in mind that the latter did not include the contribution by Type 2 quasars.

8 CONCLUSIONS

We have estimated the contribution to the infrared background and infrared number counts from AGN by using the most recent AGN luminosity functions and evolution from the hard X-ray surveys (Ueda et al. 2003) and by connecting their X-ray and IR emission by means of new detailed AGN SEDs derived by us. This approach allowed us to derive the contribution of AGN to the infrared background by using mostly observed and measured quantities, with few additional assumptions.

The main results are the following.

(i) The AGN nuclear IR radiation contributes little (<5 per cent) to the IR background at most wavelengths.

(ii) AGN along with their host galaxies contribute significantly (∼5–20 per cent) to the IR background at $\lambda < 60$ μm.

(iii) AGN and their hosts probably dominate the mid-IR number counts at bright fluxes (>1 mJy).

(iv) The predicted contribution of AGN and of their host galaxies to the mid-IR background and number counts are in good agreement with the observational constraints available so far.

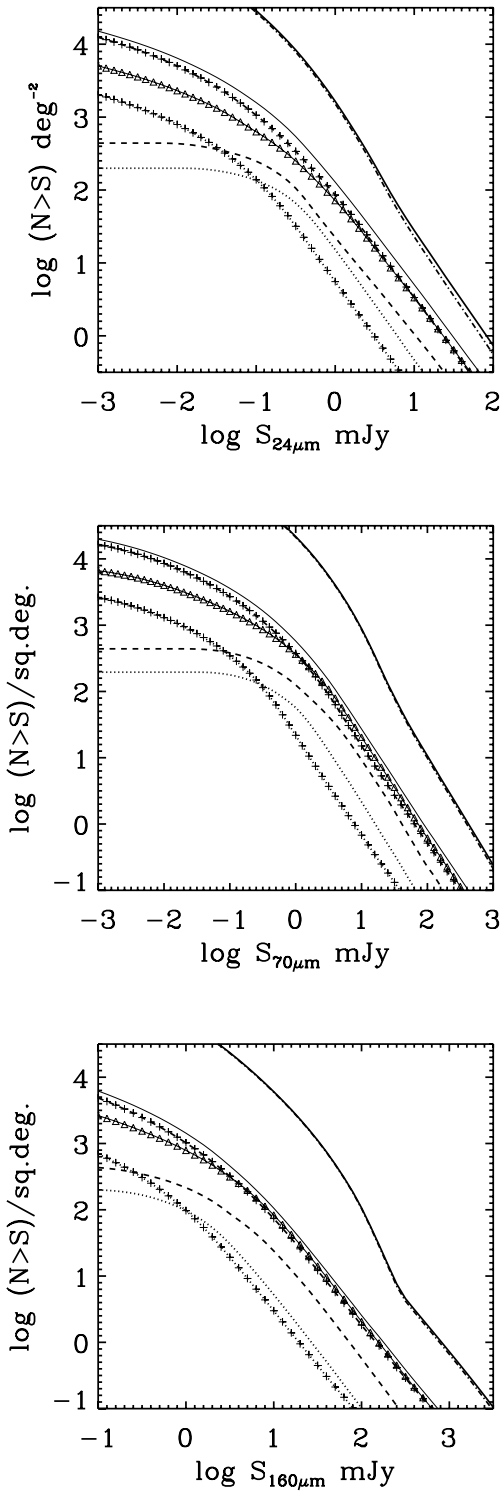

Figure 8. Number counts for AGN + hosts and galaxies in the Spitzer/MIPS bands. Meaning of lines is: thin continuous for AGN + their host galaxies; dotted and dashed for the hosts of Type 1 and 2 QSOs, respectively; the same line styles with plus signs superimposed are for Type 1 and 2 Seyferts; the connected triangles show the contribution by Compton-thick AGN ($N_{\rm H} > 10^{24}$ cm^{-2}); dot-dashed line for galaxies.

(v) However, we find a strong discrepancy between the expected contribution of Seyfert host galaxies at high redshift to the submillimetre background and number counts at bright fluxes. We ascribe this discrepancy mostly to the shortage of Seyferts at high redshift ($z \sim 2$) in the X-ray luminosity functions which, at these high redshifts and low luminosities, are still poorly constrained by the current hard X-ray surveys. This issue may also yield to an underestimate of the AGN host contribution to the far-IR bands of Spitzer. A more detailed investigation of this issue and of the possible implications for the evolution of Seyferts at high redshift will be discussed in an upcoming paper (Silva et al. in preparation).

ACKNOWLEDGMENTS

This work was partially supported by the Italian Ministry of Research (MIUR), by the National Institute for Astrophysics (INAF) and by the Italian Space Agency (ASI). LS and GLG acknowledge the kind hospitality by INAOE where part of this work was performed, and SAGG for partial financial support. We thank Fabio La Franca for useful discussions and for providing the 15-μm data in advance of publication. We thank the referee for careful reading and for many useful comments that helped us to improve the presentation.

REFERENCES

Aitken D. K., Roche P. F., 1984, MNRAS, 208, 751
Alexander D. M., Bauer F. E., Chapman S. C., Smail I., Blain A. W., Brandt W. N., Ivison R. J., 2004, in Multiwavelength Mapping of Galaxy Formation and Evolution. astro-ph/0401129
Alexander D. M. et al., 2003, AJ, 125, 383
Alonso-Herrero A., Simpson C., Ward M. J., Wilson A. S., 1998, ApJ, 495, 196
Alonso-Herrero A., Quillen A. C., Simpson C., Efstathiou A., Ward M. J., 2001, AJ, 121, 1369
Alonso-Herrero A., Quillen A. C., Rieke G. H., Ivanov V. D., Efstathiou A., 2003, AJ, 126, 81
Altieri B. et al., 1999, A&A, 343, L65
Andreani P., Cristiani S., Grazian A., La Franca F., Goldschmidt P., 2003a, AJ, 125, 444
Andreani P., Spinoglio L., Malkan M. A., 2003b, ApJ, 597, 759
Andreani P., Franceschini A., Granato G., 1999, MNRAS, 306, 161
Barger A. J., Cowie L. L., Steffen A. T., Hornschemeier A. E., Brandt W. N., Garmire G. P., 2001, ApJ, 560, L23
Barger A. J. et al., 2003, AJ, 126, 632
Bassani L., Dadina M., Maiolino R., Salvati M., Risaliti G., della Ceca R., Matt G., Zamorani G., 1999, ApJS, 121, 473
Bertin E., Dennefeld M., Moshir M., 1997, A&A, 323, 685
Brinkmann W., Grupe D., Branduardi-Raymont G., Ferrero E., 2003, A&A, 398, 81
Boisson C., Durret F., 1986, A&A, 168, 32
Boller T., Gallo L. C., Lutz D., Sturm E., 2002, MNRAS, 336, 1143
Boyle B. J., Shanks T., Croom S. M., Smith R. J., Miller L., Loaring N., Heymans C., 2000, MNRAS, 317, 1014
Brandt W. N. et al., 2001, AJ, 122, 1
Ceballos M. T., Barcons X., 1996, MNRAS, 282, 493
Cimatti A. et al., 2002, A&A, 392, 395
Comastri A., Setti G., Zamorani G., Hasinger G., 1995, A&A, 296, 1
Croom S. M. et al., 2002, MNRAS, 337, 275
Della Ceca R. et al., 2002, ApJ, 581, L9
Devereux N. A., 1989, ApJ, 346, 126
Dole H. et al., 2001, A&A, 372, 702
Efstathiou A., Rowan-Robinson M., 1995, MNRAS, 273, 649
Efstathiou A. et al., 2000, MNRAS, 319, 1169
Elbaz D. et al., 1999, A&A, 351, L37
Elvis M. et al., 1994, ApJS, 95, 1
Fadda D., Flores H., Hasinger G., Franceschini A., Altieri B., Cesarsky C. J., Elbaz D., Ferrando P., 2002, A&A, 383, 838
Ferrarese L., Merritt D., 2000, ApJ, 539, L9

Fiore F. et al., 2003, A&A, 409, 79
Frogel J. F., Elias J. H., Phillips M. M., 1982, ApJ, 260, 70
Fukazawa Y., Iyomoto N., Kubota A., Matsumoto Y., Makishima K., 2001, A&A, 374, 73
Galliano E., Alloin D., Granato E. L., Villar-Martin M., 2003, A&A, 412, 615
Gaskell C. M., Goosmann R. W., Antonucci R. R. J., Whysong D. H., 2004, ApJ, in press
George I. M., Turner T. J., Yaqoob T., Netzer H., Laor A., Mushotzky R. F., Nandra K., Takahashi T., 2000, ApJ, 531, 52
Giacconi R. et al., 2001, ApJ, 551, 624
Gilli R., Salvati M., Hasinger G., 2001, A&A, 366, 407
Glass I. S., Moorwood A. F. M., 1985, MNRAS, 214, 429
Glass I. S., Moorwood A. F. M., Eichendorf W., 1982, A&A, 107, 276
Glass I. S., 2004, MNRAS, 350, 1049
Granato G. L., Danese L., 1994, MNRAS, 268, 235
Granato G. L., Danese L., Franceschini A., 1997, ApJ, 486, 147
Granato G. L., De Zotti G., Silva L., Bressan A., Danese L., 2004, ApJ, 600, 580
Gruppioni C., Lari C., Pozzi F., Zamorani G., Franceschini A., Oliver S., Rowan-Robinson M., Serjeant S., 2002, MNRAS, 335, 831
Guainazzi M., Matt G., Brandt W. N., Antonelli L. A., Barr P., Bassani L., 2000, A&A, 356, 463
Haas M. et al., 2003, A&A, 402, 87
Haas M., Müller S. A. H., Chini R., Meisenheimer K., Klaas U., Lemke D., Kreysa E., Camenzind M., 2000, A&A, 354, 453
Hasinger G., 2003, in The Restless High-Energy Universe. astro-ph/0310804
Hasinger G. et al., 2001, A&A, 365, L45
Hauser M. G., Dwek E., 2001, ARA&A, 39, 249
Iyomoto N., Fukazawa Y., Nakai N., Ishihara Y., 2001, ApJ, 561, L69
Jaffe W. et al., 2004, Nat, 429, 47
Kauffmann G. et al., 2003, MNRAS, 346, 1055
Kochanek C. S. et al., 2001, ApJ, 560, 566
Kotilainen J. K., Ward M. J., Boisson C., Depoy D. L., Smith M. G., 1992, MNRAS, 256, 149
Krabbe A., Böker T., Maiolino R., 2001, ApJ, 557, 626
Kuraszkiewicz J. K. et al., 2003, ApJ, 590, 128
Imanishi M., Ueno S., 1999, ApJ, 527, 709
Ivanov V. D., Rieke G. H., Groppi C. E., Alonso-Herrero A., Rieke M. J., Engelbracht C. W., 2000, ApJ, 545, 190
La Franca F. et al., 2004, AJ, 127, 3075
Lawson A. J., Turner M. J. L., 1997, MNRAS, 288, 920
Lonsdale C. J., Hacking P. B., Conrow T. P., Rowan-Robinson M., 1990, ApJ, 358, 60
Lonsdale C. J. et al., 2003, PASP, 115, 897
Malizia A., Bassani L., Stephen J. B., Malaguti G., Palumbo G. G. C., 1997, ApJS, 113, 311
Malkan M. A., Stecker F. W., 2001, ApJ, 555, 64
Mainieri V., Bergeron J., Hasinger G., Lehmann I., Rosati P., Schmidt M., Szokoly G., Della Ceca R., 2002, A&A, 393, 425
Maiolino R., Rieke G. H., 1995, ApJ, 454, 95
Maiolino R., Ruiz M., Rieke G. H., Keller L. D., 1995, ApJ, 446, 561
Maiolino R., Krabbe A., Thatte N., Genzel R., 1998a, ApJ, 493, 650
Maiolino R., Salvati M., Bassani L., Dadina M., della Ceca R., Matt G., Risaliti G., Zamorani G., 1998b, A&A, 338, 781
Maiolino R., Marconi A., Oliva E., 2001, A&A, 365, 37
Maiolino R., Marconi A., Salvati M., Risaliti G., Severgnini P., Oliva E., La Franca F., Vanzi L., 2001, A&A, 365, 28
Maiolino R., 2002, Rev. Mod. Astron., 15, 179
Maiolino R. et al., 2003, MNRAS, 344, L59
Marconi A., Oliva E., van der Werf P. P., Maiolino R., Schreier E. J., Macchetto F., Moorwood A. F. M., 2000, A&A, 357, 24
Marconi A., Hunt L. K., 2003, ApJ, 589, L21
Matt G. et al., 1997, A&A, 325, L13
Matt G. et al., 1999, A&A, 341, L39
Matute I. et al., 2002, MNRAS, 332, L11
Mazzei P., Aussel H., Xu C., Salvo M., De Zotti G., Franceschini A. 2001, New Astron., 6, 265
McAlary C. W., McLaren R. A., McGonegal R. J., Maza J., 1983, ApJS, 52, 341
McLeod K. K., Rieke G. H., 1994a, ApJ, 431, 137
McLeod K. K., Rieke G. H., 1994b, ApJ, 420, 58
Minezaki T., Yoshii Y., Kobayashi Y., Enya K., Suganuma M., Tomita H., Aoki T., Peterson B. A., 2004, ApJ, 600, L35
Moustakas L. A., Davis M., Graham J. R., Silk J., Peterson B. A., Yoshii Y., 1997, ApJ, 475, 445
Nenkova M., Ivezić, Ž., Elitzur M., 2002, ApJ, 570, L9
Oliva E., Origlia L., Maiolino R., Moorwood A. F. M., 1999, A&A, 350, 9
Oliver S. J. et al., 1997, MNRAS, 289, 471
Oliver S. et al., 2002, MNRAS, 332, 536
Pearson C., Rowan-Robinson M., 1996, MNRAS, 283, 174
Perola G. C., Matt G., Cappi M., Fiore F., Guainazzi M., Maraschi L., Petrucci P. O., Piro L., 2002, A&A, 389, 802
Papadopoulos P. P., Seaquist E. R., 1999, ApJ, 514, L95
Pier E. A., Krolik J. H., 1993, ApJ, 418, 673
Quillen A. C., McDonald C., Alonso-Herrero A., Lee A., Shaked S., Rieke M. J., Rieke G. H., 2001, ApJ, 547, 129
Reeves J. N., Turner M. J. L., 2000, MNRAS, 316, 234
Reynolds C. S., 1997, MNRAS, 286, 513
Rieke G. H., 1978, ApJ, 226, 550
Risaliti G., Maiolino R., Salvati M., 1999, ApJ, 522, 157
Risaliti G., Elvis M., Gilli R., 2002, ApJ, 566, L67
Rodighiero G., Lari C., Franceschini A., Gregnanin A., Fadda D., 2003, MNRAS, 343, 1155
Sanders D. B., Mirabel I. F., 1996, ARA&A, 34, 749
Saracco P., Giallongo E., Cristiani S., D'Odorico S., Fontana A., Iovino A., Poli F., Vanzella E., 2001, A&A, 375, 1
Sato Y. et al., 2003, A&A, 405, 833
Schinnerer E., Eckart A., Tacconi L. J., Genzel R., Downes D., 2000, ApJ, 533, 850
Scoville N. Z., Becklin E. E., Young J. S., Capps R. W., 1983, ApJ, 271, 512
Serjeant S. et al., 2000, MNRAS, 316, 768
Setti G., Woltjer L., 1989, A&A, 224, L21
Severgnini P. et al., 2000, A&A, 360, 457
Siebenmorgen R., Moorwood A., Freudling W., Kaeufl H. U., 1997, A&A, 325, 450
Silva L., Granato G. L., Bressan A., Danese L., 1998, ApJ, 509, 103
Silva L., De Zotti G., Granato G. L., Maiolino R., Danese L., 2004, A&A, submitted (astro-ph/0403166)
Simpson C., 1998, ApJ, 509, 653
Spinoglio L., Andreani P., Malkan M. A., 2002, ApJ, 572, 105
Surace J. A., Sanders D. B., Evans A. S., 2001, AJ, 122, 2791
Taniguchi Y. et al., 1997, A&A, 328, L9
Telfer R. C., Zheng W., Kriss G. A., Davidsen A. F., 2002, ApJ, 565, 773
Tresch-Fienberg R., Fazio G. G., Gezari D. Y., Lamb G. M., Shu P. K., Hoffmann W. F., McCreight C. R., 1987, ApJ, 312, 542
Totani T., Yoshii Y., Maihara T., Iwamuro F., Motohara K., 2001, ApJ, 559, 592
Turner T. J., George I. M., Nandra K., Turcan D., 1999, ApJ, 524, 667
Ueda Y., Akiyama M., Ohta K., Miyaji T., 2003, ApJ, 598, 886
Vanden Berk D. E. et al., 2001, AJ, 122, 549
Vignali C., Comastri A., 2002, A&A, 381, 834
Ward M., Allen D. A., Wilson A. S., Smith M. G., Wright A. E., 1982, MNRAS, 199, 953
Ward M., Elvis M., Fabbiano G., Carleton N. P., Willner S. P., Lawrence A., 1987, ApJ, 315, 74
Wright G. S., Joseph R. D., Robertson N. A., James P. A., Meikle W. P. S., 1988, MNRAS, 233, 1

APPENDIX A: THE SAMPLES USED TO DERIVE SPECTRAL ENERGY DISTRIBUTIONS

In Tables A1–A3 we list the samples of Sy1s, Sy2s and QSOs, respectively, used to derive the IR SEDs discussed in Sections 3 and 4. The tables report the *intrinsic* hard X-ray luminosities (i.e. corrected for absorption), the nuclear IR luminosities inferred by our nuclear SEDs, and the total IR luminosities (i.e. AGN + host). For Sy1s and QSOs we also report the luminosity of the UV–optical bump inferred by adapting the combined average SED of Type 1 AGN obtained by Vanden Berk et al. (2001) and by Telfer et al. (2002) (the latter for the extreme UV part of the spectrum) to the optical nuclear photometric points (either from *HST* or from high-resolution ground-based optical observations).

The sample and IR SED of Compton-thick Sy2s with $10^{24} < N_{\rm H} < 10^{25}\,{\rm cm}^{-2}$ deserves more discussion. Near-infrared observations of this class of object rarely shows indication of non-stellar emission, strongly suggesting that heavy dust obscuration in these objects often prevents the detection of the nuclear near-IR source. Of the five Sy2s in this $N_{\rm H}$ range only two (namely NGC 3281 and Circinus) show clear evidence for near-IR non-stellar emission. For these we could fit the Granato & Danese (1994) models to the data and derive their nuclear IR SED. However, most likely these two objects represent the less absorbed cases of this class, therefore providing a biased view of their SED. Therefore we tried to account also for the SED of the more obscured AGN. In the other three sources with $10^{24} < N_{\rm H} < 10^{25}\,{\rm cm}^{-2}$ (namely NGC 4945, 3079, 5194) there is probably a detection of the obscured AGN only at 10 μm (e.g. Krabbe, Böker & Maiolino 2001). We used the IR SED determined for Circinus and NGC 3281, normalized to the X-ray intrinsic flux of the three sources and then increased the obscuration of the Granato & Danese (1994) model (by increasing the inclination angle of the torus) until the SED matched the observed 10-μm nuclear photometry, with the additional constraint that the integrated nuclear IR emission should not change. This is a rough method to include the SED of the very obscured AGN with $10^{24} < N_{\rm H} < 10^{25}\,{\rm cm}^{-2}$, but it is the best guess that can be made with the available data.

All the average SEDs obtained in this paper are available in electronic form at the following web site: http://www.arcetri.astro.it/∼maiolino/agnsed.

Table A1. Sample of Seyfert 1 galaxies.

Name	z	lg $L^{a}_{2-10\,{\rm keV}}$	lg $L_{\rm IR}$(nuc)^{a,b}	lg $L_{\rm IR}$(tot)^{a,c}	lg $L_{\rm UV-opt}$(nuc)^{a,d}	Refs.(X)^{e}	Refs.(IR)^{f}
NGC 3227	0.0039	41.9	42.3	42.6	43.5	1	1,2,3
NGC 3516	0.0088	43.1	42.7	43.3	43.8	1	4
NGC 3783	0.0097	43.0	43.2	43.4	43.9	1	5,6,7
NGC 4051	0.0023	41.3	41.9	42.1	42.0	1	4
NGC 4151	0.0033	42.7	43.0	42.4	43.2	2	1,8
NGC 4253	0.0129	42.2	43.2	43.6	44.0	3	4
NGC 4593	0.009	42.8	42.9	43.3	43.1	4	9,10,5,11,12,8
NGC 5548	0.0172	43.4	43.5	43.9	44.4	4	1,13,9
NGC 7213	0.0039	42.1	42.2	42.6	43.1	5	10,14,15
NGC 7469	0.0163	43.3	44.2	43.8	45.0	4	1,2,8
IC 4329	0.016	43.8	44.0	43.8	45.2	1	1,8
Mrk 1095	0.0323	44.0	43.8	44.4	–	3	5,6,8
Mrk 1513	0.0629	43.6	44.4	45.0	45.5	6	4
Mrk 335	0.0258	43.1	43.6	44.2	44.7	1	4
Mrk 590	0.0263	43.6	43.5	44.2	44.1	4	4
Mrk 841	0.0129	42.6	43.2	43.6	43.6	7	4
MCG-6-30-15	0.0077	42.8	42.9	43.2	43.4	1	5,8,11

[a] All luminosities are in units of erg s^{-1}.

[b] Nuclear infrared luminosity associated with dust emission heated by the AGN calculated in the range 8–1000 μm for comparison in $L_{\rm IR}$ defined by Sanders & Mirabel (1996).

[c] Total (AGN + host) infrared luminosity in the range 8–1000 μm estimated by using the IRAS data and following the prescription in Sanders & Mirabel (1996).

[d] Luminosity of the UV-optical blue bump of the AGN (see text).

[e] References for the X-ray data: (1) Reynolds (1997), (2) Malizia et al. (1997), (3) Turner et al. (1999), (4) Perola et al. (2002), (5) Imanishi & Ueno (1999), (6) Lawson & Turner (1997), (7) Ceballos & Barcons (1996).

[f] References for the nuclear IR data: (1) Alonso-Herrero et al. (2001), (2) Krabbe et al. (2001), (3) Wright et al. (1988), (4) Alonso-Herrero et al. (2003), (5) Oliva et al. (1999), (6) McAlary et al. (1983), (7) Frogel et al. (1982), (8) Ward et al. (1987), (9) Quillen et al. (2001) (10) Kotilainen et al. (1992) (11) Glass & Moorwood (1985) (12) Maiolino et al. (1995) (13) Rieke (1978) (14) Ward et al. (1982) (15) Glass, Moorwood & Eichendorf (1982).

Table A2. Sample of Seyfert 2 galaxies.

Name	z	$N_{\rm H}{}^{a}$	lg $L_{2-10\,{\rm keV}}{}^{b,c}$	lg $L_{\rm IR}({\rm nuc})^{b,d}$	lg $L_{\rm IR}({\rm tot})^{b,e}$	Refs.(X)^{f}	Refs.(IR)^{g}
NGC 1365	0.005457	20^{+4}_{-4}	42.1	42.6	44.8	2	5,6,7,8
NGC 3079	0.006	1000^{+540}_{-530}	42.5	42.6	44.6	3	15
NGC 3081	0.007955	64^{+20}_{-12}	42.4	42.7	42.1	4	10,11,12,13
NGC 3281	0.01067	196^{+19}_{-5}	43.2	43.6	44.4	5	14,9,13
NGC 4388	0.008419	42^{+6}_{-10}	42.8	42.6	44.2	2	10,11,16,17
NGC 4945	0.00093	400^{+20}_{-12}	41.6	41.5	43.9	6	9
NGC 5194	0.00093	560^{+40}_{-16}	40.6	40.6	43.2	7	20
NGC 5252	0.00618	$4.3^{+0.6}_{-0.6}$	41.9	41.7	41.9	2	1,21
NGC 5506	0.00618	$3.4^{+0.3}_{-0.1}$	42.9	43.1	44.0	2	1,18
NGC 5674	0.0249	$7.0^{+2.8}_{-2.6}$	43.2	43.1	44.4	2	10,16,19,20
NGC 7172	0.00868	$8.6^{+0.8}_{-0.3}$	42.5	42.8	44.0	2	1,21
NGC 7582	0.00528	$12.4^{+0.6}_{-0.8}$	42.5	42.9	44.4	2	10,22,5,6,7
Mrk 348	0.015	$10.6^{+3.1}_{-2.6}$	43.0	43.5	44.0	2	1,23
Circinus	0.00093	430^{+40}_{-70}	41.9	42.6	43.7	8	10,24,25,9
MGC-5-23-16	0.0082	$1.6^{+0.2}_{-0.2}$	43.1	43.3	42.2	2	1,7

[a] Intrinsic absorbing column density in units of 10^{22} cm^{-2}.
[b] All luminosities are in units of erg s^{-1}.
[c] The hard X-ray lumionsity is corrected for absorption.
[d] Nuclear infrared luminosity associated with dust emission heated by the AGN calculated in the range 8–1000 μm for comparison in $L_{\rm IR}$ defined by Sanders & Mirabel (1996).
[e] Total (AGN + host) infrared luminosity in the range 8–1000 μm estimated by using the IRAS data and following the prescription in Sanders & Mirabel (1996).
[f] References for the X-ray data: (1) Matt et al. (1997), (2) Bassani et al. (1999), (3) Iyomoto et al. (2001), (4) Maiolino et al. (1998b), (5) Vignali & Comastri (2002), (6) Guainazzi et al. (2000), (7) Fukazawa et al. (2001), (8) Matt et al. (1999).
[g] References for the nuclear IR data: (1) Alonso-Herrero et al. (2001), (2) Tresch-Fienberg et al. (1987), (3) Papadopoulos & Seaquist (1999), (4) Schinnerer et al. (2000), (5) Oliva et al. (1999), (6) McAlary et al. (1983), (7) Frogel, Elias & Phillips (1982), (8) Devereux (1989), (9) Krabbe et al. (2001), (10) Quillen et al. (2001) (11) Alonso-Herrero et al. (1998), (12) Ward et al. (1982) (13) Boisson & Durret (1986) (14) Simpson (1998) (15) Alonso-Herrero et al. (2003), (16) McLeod & Rieke (1994a), (17) Scoville et al. (1983), (18) Ward et al. (1987), (19) Ivanov et al. (2000), (20) Maiolino et al. (1995), (21) Aitken & Roche (1984), (22) Kotilainen et al. (1992) (23) Rieke (1978) (24) Maiolino et al. (1998a) (25) Siebenmorgen et al. (1997) (26) Glass et al. (1982).

Table A3. Sample of quasars.

Name	z	lg $L^{a}_{2-10\,{\rm keV}}$	lg $L_{\rm IR}({\rm tot})^{a,b}$	lg $L_{\rm UV-opt}{}^{a,c}$	Refs.(X)^{d}
PG0050+124	0.06	43.7	45.5	45.4	1
PG0054+144	0.17	44.3	45.5	45.7	1
PG0157+001	0.16	44.8	46.2	45.6	2
Q0710+45	0.05	44.3	45.0	45.2	3
PG0804+761	0.1	44.2	45.0	45.6	4
Q0844+34	0.06	43.3	44.7	45.2	5
PG1211+143	0.08	44.0	45.2	45.6	1
PG1307+085	0.1	44.1	44.7	45.5	6
IRAS13349+2438	0.1	44.4	45.8	45.5	1
PG1426+015	0.08	43.8	45.0	45.4	6
PG1440+356	0.07	43.8	45.0	45.3	1
PG1613+658	0.12	44.3	45.5	45.6	6
E1821+643	0.29	45.5	46.5	46.8	1
PG2130+099	0.06	43.5	45.0	45.3	6

[a] All luminosities are in units of erg s^{-1}.
[b] Total (AGN + host) infrared luminosity in the range 8–1000 μm estimated by using the IRAS data and following the prescription in Sanders & Mirabel (1996).
[c] Luminosity of the UV–optical blue bump of the AGN (see text).
[d] References for the X-ray data: (1) Reeves & Turner (2000), (2) Boller et al. (2002), (3) Ceballos & Barcons (1996), (4) George et al. (2000), (5) Brinkmann et al. (2003), (6) Lawson & Turner (1997).

This paper has been typeset from a TEX/LATEX file prepared by the author.